GEOLOGY | THE GEOLOGICAL SOCIETY OF AMERICA®

https://doi.org/10.1130/G47961.1

Manuscript received 1 June 2020
Revised manuscript received 21 July 2020
Manuscript accepted 27 July 2020

Permian plume-strengthened Tarim lithosphere controls the Cenozoic deformation pattern of the Himalayan-Tibetan orogen

Xi Xu[1,2,3], Andrew V. Zuza[4], An Yin[3], Xiubin Lin[1], Hanlin Chen[1]* and Shufeng Yang[1]

[1]Key Laboratory of Geoscience Big Data and Deep Resource of Zhejiang Province, School of Earth Sciences, Zhejiang University, Hangzhou 310027, China

[2]China Aero Geophysical Survey and Remote Sensing Center for Natural Resources, China Geological Survey, Beijing 100083, China

[3]Department of Earth, Planetary, and Space Sciences, University of California–Los Angeles, Los Angeles, California 90095-1567, USA

[4]Nevada Bureau of Mines and Geology, University of Nevada, Reno, Nevada 89557, USA

ABSTRACT

The high strength of the Tarim Basin (northwestern China) lithosphere, widely regarded as a Precambrian craton, is evidenced by its resistance to Cenozoic deformation in the Himalayan-Tibetan orogen. However, Neoproterozoic suturing and early Paleozoic shortening within the Tarim Basin suggest that its rigidity is a relatively recent phenomenon with unknown cause. We reprocessed high-resolution magnetic data that show a 300–400-km-diameter radial pattern of linear anomalies emanating from a central region characterized by mixed positive-negative anomalies. We suggest that this pattern was generated by the previously hypothesized Permian (ca. 300–270 Ma) plume beneath the Tarim Basin. Constrained by published geochemical and geochronological data from plume-related igneous rocks, we propose that the ~30 m.y. Permian plume activity resulted in a more viscous, depleted, thicker, dehydrated, and low-density mantle lithosphere. The resulting stronger lithosphere deflected strain from the Cenozoic India-Asia convergence around Tarim Basin, including Pamir overthrusting to the northwest and Altyn Tagh left-slip displacement to the northeast, thus shaping the geometry of the Himalayan-Tibetan orogen.

INTRODUCTION

The interior of the Tarim Basin, northwestern China, has remained undeformed during the development of the Cenozoic Himalayan-Tibetan orogen, expressed by flat-lying Cenozoic strata (e.g., Jia, 1997). Although its rigidity has been attributed to the presence of Precambrian basement (e.g., Neil and Houseman, 1997), this is inconsistent with the observation of an early Paleozoic thrust belt developed across the Tarim Basin (e.g., Yin and Nie, 1996; Jia, 1997; Carroll et al., 2001), which requires the acquisition of greater strength to resist Cenozoic deformation between the early Paleozoic and end of the Mesozoic. Alternatively, the rigidity of the Tarim lithosphere could have developed via the presence of a Precambrian oceanic plateau that was strengthened from below by a Permian plume (e.g., Deng et al., 2017). This model implies that Tarim was already strong prior to the Phanerozoic, inconsistent with aforementioned Paleozoic shortening across the basin. Because Early Permian (ca. 300–270 Ma) mafic magmatism, interpreted to have been derived from a plume (Yang et al., 1996; Chen et al., 2006; Xu et al., 2014), was the only regionally extensive event affecting the Tarim Basin after the early Paleozoic (e.g., Jia, 1997; Carroll et al., 2001; Guo et al., 2005), it is possible that plume-induced processes profoundly strengthened the earlier Tarim mantle lithosphere. Assessing this possibility requires a sound knowledge of the root zone of the plume, which is obscured by ~10 km of overlying Mesozoic–Cenozoic strata (Jia, 1997; Guo et al., 2005).

Aeromagnetic anomalies have proven to be effective in locating and quantifying the geometry and extent of mafic intrusions associated with a mantle plume (e.g., Finn and Morgan, 2002). The success of this approach inspired us to reexamine the aeromagnetic data across Tarim. The extent of Permian intrusive rocks beneath the Tarim cover sequence has never been systematically determined before with aeromagnetic data sets (e.g., Xiong et al., 2016). Our reprocessed data reveal a 300–400-km-diameter radial pattern of magnetic lineaments that emanate from a central region characterized by mixed positive and negative anomalies. Constrained by the existing geochemical and geochronological data from the plume-related igneous rocks, we argue that Tarim's mantle lithosphere was thickened, depleted, and dehydrated by the Permian plume to transform Tarim into a rigid craton-like continent in situ through the development of a thick mantle keel and input of mafic intrusions into the crust (e.g., Lee et al., 2011). Tarim's stronger lithosphere deflected strain from Cenozoic India-Asia convergence around the Tarim Basin to shape the deformation pattern of the Himalayan-Tibetan orogen.

GEOLOGICAL SETTING

The Precambrian basement of the Tarim Basin consists of continental blocks that amalgamated along the Neoproterozoic central Tarim suture zone (Guo et al., 2005; Yang et al., 2018). The margins of the Tarim Basin were affected episodically by arc development and arc-continent collision throughout the Paleozoic during the development and closure of the Paleo-Asian oceans to the north (i.e., present southern Tian Shan; e.g., Yin and Nie, 1996; Xiao et al., 2005), and the Tethyan oceans to the south (i.e., present Tibetan Plateau; e.g., Yin and Harrison, 2000; Wu et al., 2016). The subduction polarity of the Carboniferous–Permian arc systems is enigmatic due to poor exposure and Cenozoic modification, but based on correlative subduction systems to the east (e.g., Xiao et al., 2003; Wu et al., 2016), there is a strong possibility that both subduction systems dipped beneath the Tarim continent.

*E-mail: hlchen@zju.edu.cn

CITATION: Xu, X., et al., 2020, Permian plume-strengthened Tarim lithosphere controls the Cenozoic deformation pattern of the Himalayan-Tibetan orogen: Geology, v. 49, p. , https://doi.org/10.1130/G47961.1

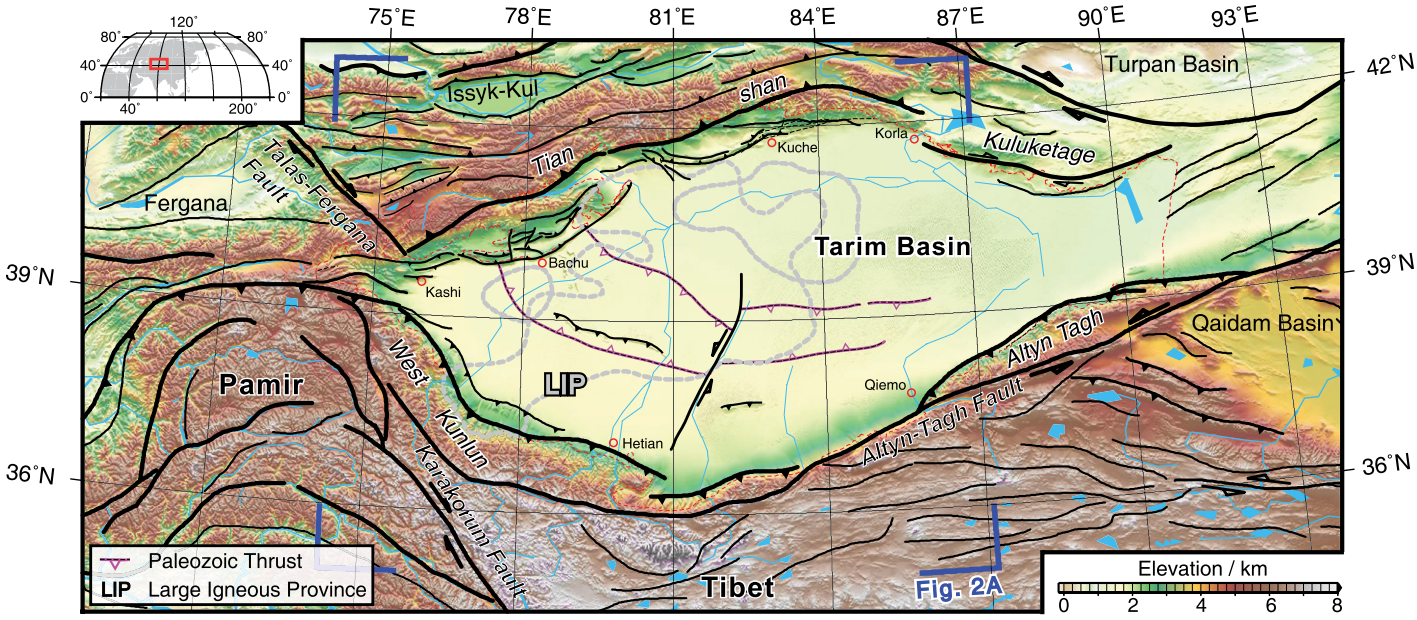

Figure 1. Topographic and tectonic map of the Tarim Basin (northwestern China). Early Paleozoic thrusts are after Jia (1997) and Yin and Nie (1996).

The Tarim Basin's interior was affected by two regional events in the Phanerozoic. The first occurred in the early Paleozoic, expressed by reactivation of the Neoproterozoic suture zone as evidenced by thrusting and folding (Fig. 1; Jia, 1997; Carroll et al., 2001; Guo et al., 2005), which was coeval with the closure of the Qilian and Kunlun oceans in northern Tibet (Wu et al., 2016). The second event occurred during the Early Permian (300–270 Ma), expressed as widespread igneous activity, defining a large igneous province (LIP), possibly induced by a mantle plume from below (Chen et al., 2006; Xu et al., 2014). The full extent of the LIP is obscured by a >~10 km section of sedimentary cover, but its wide distribution is indicated by surface exposures, subsurface samples, and extrapolation of these findings by analysis and interpretation of available seismic reflection profiles (Fig. 2A; e.g., Xu et al., 2014). The Permian plume-head location has been variably assigned to the Tian Shan and southwestern or northern Tarim (Chen et al., 2006; Li et al., 2014; Liu et al., 2016; Cheng et al., 2018). Subsequent Cenozoic India-Asia convergence resulted in concentrated shortening along the margins of Tarim Basin, including thin-skinned thrust belts in the north and west and strike-slip faulting in the southeast (Fig. 1; Yin et al., 1998; Guo et al., 2005).

PERMIAN PLUME HEAD

Data used in this study are mainly from the aeromagnetic data set of China (Xiong et al., 2016) with a 1 km × 1 km grid spacing and 1 km datum, supplemented by the Earth Magnetic Anomaly Grid Version 2 (EMAG2; Maus et al., 2009; see also Fig. S1A in the Supplemental Material[1]). The combined data set was first processed by reduction to pole (Fig. S2; e.g., Arkani-Hamed, 1988) and next by analytical signal transformation (Fig. S3; see details in the Supplemental Material; Roest et al., 1992). A series of high-amplitude, long-wavelength anomalies are superimposed by four variably oriented, short-wavelength, positive linear anomalies across the northwestern Tarim Basin (e.g., the Bachu Uplift; i.e., L1–L4 in Fig. S2). High-amplitude, long-wavelength magnetic anomalies have previously been correlated to signals derived from the Tarim Precambrian crystalline basement (e.g., Xiong et al., 2016; Yang et al., 2018). The final reprocessed result (Fig. 2A) reveals a radial pattern of linear anomalies: L1 lineaments trend southeast, L2 lineaments trend east and southeast, L3 lineaments trend east, and L4 lineaments trend northeast (Fig. 2A; Fig. S3), converging near Bachu City (~39.8°N, ~78.6°E).

The radial linear anomalies overlap the Permian volcanic field (Fig. 2A). They converge beneath the observed ca. 300 Ma kimberlite complex, which are the oldest Permian intrusive rocks in Tarim Basin that are proposed to be associated with, and derived from, the plume head (Fig. 2A; e.g., Chen et al., 2006; Xu et al., 2014). This spatial correlation led us to interpret the linear magnetic anomalies to represent a giant dike swarm with arms radiating ~150–200 km outward from the center interpreted as the Permian plume head. Additionally, isolated magnetic highs dispersed across Tarim Basin may have been related to plume-induced mafic intrusions (Fig. 2A).

To assess whether the linear anomalies are related to Permian intrusions, we compiled 25,643 detailed rock-magnetic susceptibility measurements from within and around the Tarim Basin (Table S1). The measured susceptibilities concentrated in the Permian igneous suites range from ~27×10^{-5} to ~$11{,}700 \times 10^{-5}$ SI, with high mean values (>5300×10^{-5} SI; Fig. S1B). The high values of Permian intrusions show that the radial pattern of the positive linear anomalies can indeed be explained by Permian mafic intrusions, corroborated by surface exposures and drill core (Fig. S4).

Although radially trending dikes should be distributed symmetrically around a plume center (Ernst and Buchan, 2003), our observed radial magnetic lineaments appear to occur only on the east side of the interpreted plume head. We note that the interpreted plume head is close to the southern Cenozoic Tian Shan thrust belt (Figs. 2B and 2C), which could have obscured the projected radial dikes northwest of the inferred plume head. To test this possibility, we schematically restored 20%–30% crustal shortening across the southern Tian Shan thrust belt and 10% shortening across the Tarim Basin (Fig. S5; e.g., Yin et al., 1998). This simple exercise yielded a magnetic anomaly pattern consistent with a radial dike swarm around the interpreted central plume head (Figs. 2C and 2D).

The impact and extent of the interpreted Permian plume have been constrained by the Carboniferous-Permian unconformity in the Tarim Basin (Figs. 3A and 3B; Chen et al., 2006; Li et al., 2014; Xu et al., 2014). The extent of this unconformity overlaps our interpreted region affected by the plume. Because the aeromagnetic

[1]Supplemental Material. Geochemical compilation and details for magnetic data processing, plume-head restoration, and rheological profiles. Please visit https://doi.org/10.1130/GEOL.S.12869684 to access the supplemental material, and contact editing@geosociety.org with any questions.

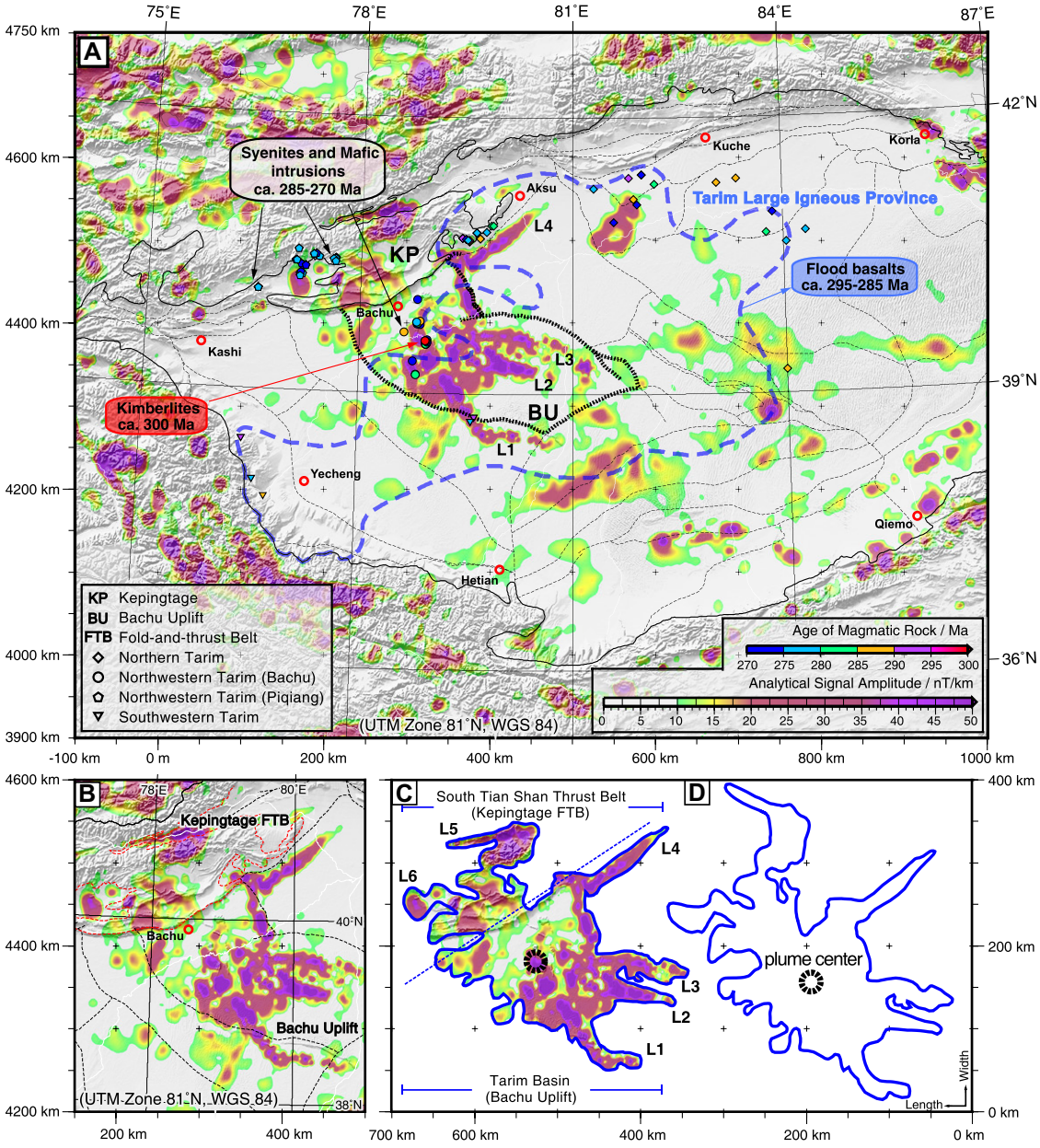

Figure 2. (A) Analytical signal of aeromagnetic anomalies in the Tarim Basin, northwestern China. Plotted symbols are from 91 samples with radiometric ages (see sources in Table S2 [see footnote 1]). Note radial lineaments, L1–L4. Thin dashed black lines are boundaries of structural units within the Tarim Basin. (B) Close-up distribution of radial signal anomalies. (C) Original morphology of imaged plume and interpreted lineaments L5–L6, and (D) restoration of Cenozoic deformation (e.g., Fig. S5). UTM—Universal Transverse Mercator; WGS 84—World Geodetic System 1984.

image of the plume is the integrated effect of intrusions in the Tarim crust, whereas the unconformity occurred over the life span of plume activity, this spatial coincidence of the two patterns suggests a relatively simple plume structure expressed by a center with a radial dike swarm that was relatively stationary, at least within the resolution of the two data sets. Within this resolution, a minor shift of the plume head is permissible (Fig. 2; Li et al., 2014), possibly facilitated by the plume exploring a preexisting weakness in the Tarim lithosphere (Liu et al., 2016). The 300–400 km plume-head diameter observed in the middle-upper crust (above the Curie surface; Fig. 2) is consistent with a plume that flattened with a >500 km diameter at the base of the lithosphere (Ernst and Buchan, 2003).

Carboniferous–Triassic inward-dipping subduction along Tarim's northern and southern margins (e.g., Xiao et al., 2005; Wu et al., 2016) was contemporaneous with plume activity (Fig. 3). The temporal and spatial overlap of subduction and the plume suggests a complex causal relationship, possibly involving flow through or around slab windows/tears, as has been hypothesized for Yellowstone and the backarc of the Patagonian Andes (e.g., Gorring et al., 1997; Kincaid et al., 2013). The exact connection between the plume and these subduction systems remains to be explored.

LITHOSPHERE STRENGTHENING BY PLUME ACTIVITY

Plume-lithosphere interactions may either destroy strong cratons (e.g., Hu et al., 2018) or strengthen the mantle lithosphere by developing a craton-like mantle keel (Lee et al., 2001, 2011). The low heat flow and resistance to Cenozoic deformation in the Tarim Basin may be explained by plume-induced lithospheric strengthening. Here, we argue that the Permian plume transformed Tarim into a stable craton-like continent in situ (Lee et al., 2011) by simultaneously building a strong mantle keel beneath Tarim and adding voluminous strong mafic rocks to the lower crust.

As outlined above, the Tarim lithosphere was not strong prior to Permian plume impingement. Permian volcanic rocks were initially derived from volatile-rich metasomatized mantle lithosphere (Zhang et al., 2013; Cheng et al., 2018), which may reflect Tarim's pre-Mesozoic subduction history (e.g., Guo et al., 2005). However, the subtle arc-subduction signature in the plume-derived melts diminished in both time, after initial ca. 300 Ma impingement, and space, moving toward the plume center (see Fig. S6

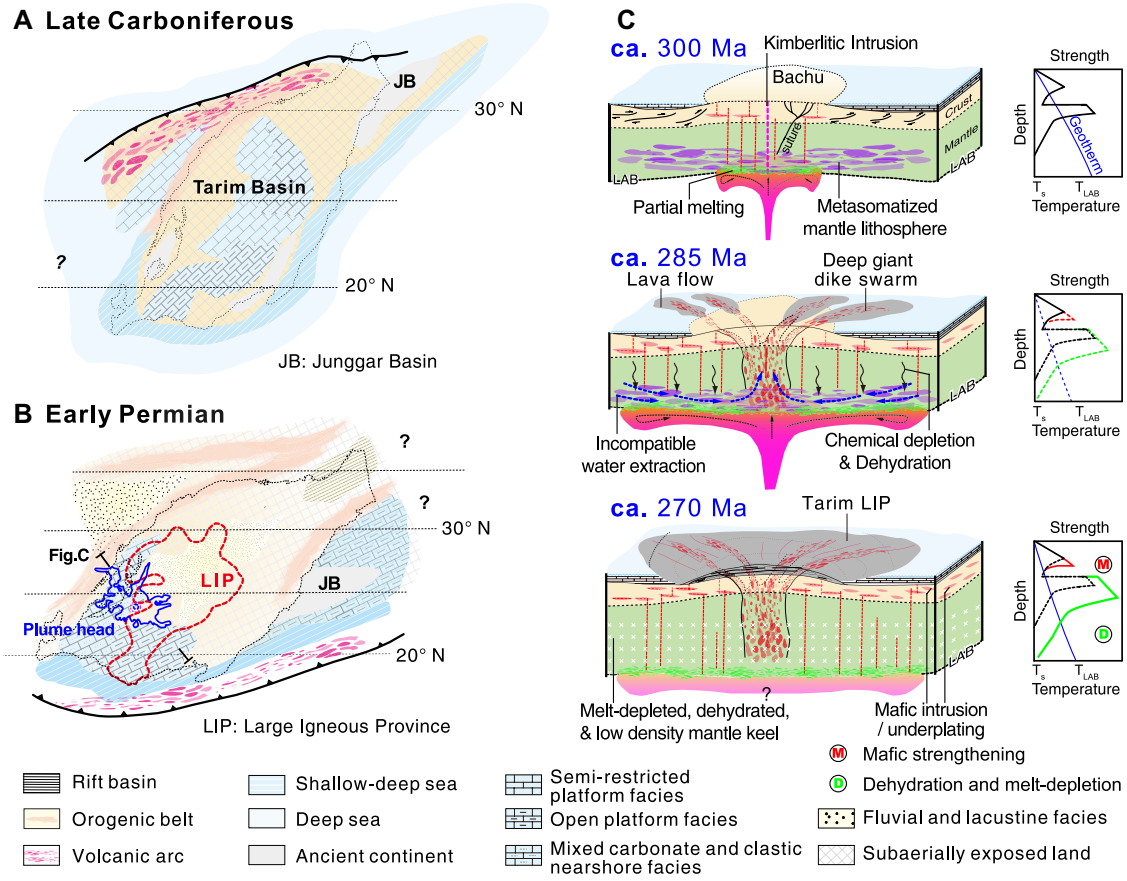

Figure 3. Model of the Tarim Permian mantle plume. (A–B) Paleogeography (Chen et al., 2006; Li et al., 2014) with plume head imaged from this study. (C) Block models of plume evolution with corresponding schematic lithospheric strength profiles and geotherm. The plume impinged on previously deformed continental lithosphere beneath the Bachu Uplift, followed by large igneous province (LIP) volcanism. Plume process modified crustal strength, with mafic intrusions and underplating, and the mantle via mantle dehydration and melt depletion. Mantle lithosphere was thickened and strengthened, constructing Tarim as a strong low-heat-flow continent. Geotherm connects the surface temperature (T_s) to fixed lithosphere-asthenosphere boundary (LAB) temperature (T_{LAB}; see details in the Supplemental Material [see footnote 1]).

for geochemical compilation). For example, Nb depletion tracked inversely by Nb/Yb ratios, commonly associated with subduction-zone influence, diminishes moving toward the plume center (Nb/Yb = 5–10 to ~20–40; Fig. S6). We interpret this trend to reflect more direct plume-derived mantle melts above the plume-head center, as opposed to mixed-source melts. At a given regional location, Nb/Yb increases through time from ca. 300 (Nb/Yb ~7) to ca. 270 Ma (Nb/Yb ~20–40; Fig. S6), which may reflect progressive dehydration/modification of the mantle lithosphere that removed the subduction-influenced signature to yield more classic ocean-island basalt (OIB) geochemistry.

Hot plume activity (zircon saturation temperatures >800 °C; Xu et al., 2014) affected the Tarim Basin for ~30 m.y. (Fig. 3), and the high heat flux would have led to high-degree partial melting, devolatilization, and thickening of the mantle lithosphere (Fig. 3C; Fig. S7). Specifically, chemical-melt depletion (e.g., Fe relative to Mg) lowered mantle density and facilitated growth of the mantle lithosphere into thickened buoyant mantle (Lee et al., 2001). Water is highly incompatible during melting, and plume magmatism dehydrated the mantle lithosphere, generating hydrated flood basalts (5 wt% H_2O; Selway et al., 2014; Liu et al., 2017). This process would have greatly strengthened the mantle lithosphere, given the inverse dependence of mantle viscosity on water content (Hirth and Kohlstedt, 1996).

Dehydration and chemical depletion together intrinsically strengthened the mantle keel. Injected and underplated mafic intrusions in the lower crust further increased crustal strength (Liu and Furlong, 1994). The flattened plume head may have been >500 km in diameter (Ernst and Buchan, 2003), and isolated signal highs across the basin (Fig. 2A) suggest a greater area was affected by the plume. With minor plume migration, as discussed above, most of the Tarim Basin may have experienced the thermal pulse associated with this plume.

These integrated contributions built Tarim into a rigid craton-like continent in the Permian (Fig. 3C). Prior to the Cenozoic, much of Tibet and the Pamirs involved arc subduction and collisional systems between various terranes (Yin and Harrison, 2000; Wu et al., 2016) that led to broad-scale hydrologic weakening of most of the region. This explains why deformation was distributed thousands of kilometers inboard of the collisional front shortly after collision (Chen and Gerya, 2016). The stronger Tarim craton-like lithosphere deflected strain from Cenozoic India-Asia convergence around the Tarim Basin, including Pamir overthrusting to the northwest and Altyn Tagh left-slip displacement to the northeast.

The Sichuan Basin also behaved rigidly within the Pamir-Tibet orogen, and the region experienced hydrated LIP volcanism (2–4 wt% H_2O; Liu et al., 2017) associated with a mantle plume at ca. 260 Ma that may have dehydrated, melt-depleted, and strengthened Sichuan's

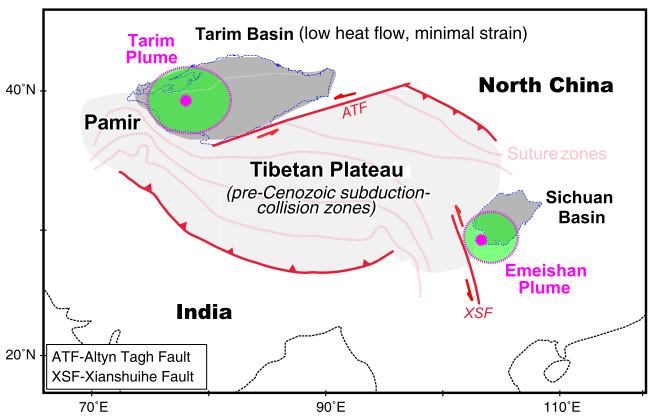

Figure 4. Sketch showing how the Tarim and Sichuan Basins may have been strengthened by Permian plumes. Suture zones and faults are after Yin and Harrison (2000) and Wu et al. (2016).

mantle. Voluminous mafic intrusions and underplating would have simultaneously strengthened the lower/middle crust. Accordingly, rheological conditioning by Permian mantle plumes may have exerted a first-order control on strain partitioning between deformed Tibetan lithosphere and the stronger Tarim and Sichuan Basins, which acted as conjugate rigid buttresses, thus shaping the geometry of the Tibetan Plateau (Fig. 4).

ACKNOWLEDGMENTS

We appreciate Shengqing Xiong for compiling aeromagnetic data in China, and Lin Chen for discussion. This work was supported by the National Natural Science Foundation of China (grants 41720104003 and 41902202), the U.S. National Science Foundation (EAR-1914501), the National Science and Technology Major Project of China (grants 2017ZX05008001 and 2016ZX05003001), the Chinese Postdoctoral Science Foundation (grant 2019M652062), and the Second Tibetan Plateau Scientific Expedition and Research (grant 2019QZKK00708). Reviews by Alex Robinson, Jay Chapman, and two anonymous reviewers greatly improved this paper. We appreciate the manuscript handling by editor Chris Clark.

REFERENCES CITED

Arkani-Hamed, J., 1988, Differential reduction-to-the-pole of regional magnetic anomalies: Geophysics, v. 53, p. 1592–1600, https://doi.org/10.1190/1.1442441.

Carroll, A.R., Graham, S.A., Chang, E.Z., and McKnight, C., 2001, Sinian through Permian tectonostratigraphic evolution of the northwestern Tarim Basin, China, *in* Hendrix, M.S., and Davis, G.A., eds., Paleozoic and Mesozoic Tectonic Evolution of Central and Eastern Asia: From Continental Assembly to Intracontinental Deformation: Geological Society of America Memoir 194, p. 47–70, https://doi.org/10.1130/0-8137-1194-0.47.

Chen, H.L., Yang, S.F., Wang, Q.H., Luo, J.C., Jia, C.Z., Wei, G.Q., Li, Z., He, G., and Hu, A.P., 2006, Sedimentary response to the Early-Mid-Permian basaltic magmatism in the Tarim plate: Geology in China, v. 33, p. 545–555.

Chen, L., and Gerya, T.V., 2016, The role of lateral lithospheric strength heterogeneities in orogenic plateau growth: Insights from 3-D thermomechanical modeling: Journal of Geophysical Research: Solid Earth, v. 121, p. 3118–3138, https://doi.org/10.1002/2016JB012872.

Cheng, Z.G., Zhang, Z.C., Xie, Q.H., Hou, T., and Ke, S., 2018, Subducted slab-plume interaction traced by magnesium isotopes in the northern margin of the Tarim Large Igneous Province: Earth and Planetary Science Letters, v. 489, p. 100–110, https://doi.org/10.1016/j.epsl.2018.02.039.

Deng, Y.F., Levandowski, W., and Kusky, T., 2017, Lithospheric density structure beneath the Tarim Basin and surroundings, northwestern China, from the joint inversion of gravity and topography: Earth and Planetary Science Letters, v. 460, p. 244–254, https://doi.org/10.1016/j.epsl.2016.10.051.

Ernst, R.E., and Buchan, K.L., 2003, Recognizing mantle plumes in the geological record: Annual Review of Earth and Planetary Sciences, v. 31, p. 469–523, https://doi.org/10.1146/annurev.earth.31.100901.145500.

Finn, C.A., and Morgan, L.A., 2002, High-resolution aeromagnetic mapping of volcanic terrain, Yellowstone National Park: Journal of Volcanology and Geothermal Research, v. 115, p. 207–231, https://doi.org/10.1016/S0377-0273(01)00317-1.

Gorring, M.L., Kay, S.M., Zeitler, P.K., Ramos, V.A., Rubiolo, D., Fernandez, M.I., and Panza, J.L., 1997, Neogene Patagonian plateau lavas: Continental magmas associated with ridge collision at the Chile triple junction: Tectonics, v. 16, p. 1–17, https://doi.org/10.1029/96TC03368.

Guo, Z.J., Yin, A., Robinson, A., and Jia, C.Z., 2005, Geochronology and geochemistry of deep-drill-core samples from the basement of the central Tarim Basin: Journal of Asian Earth Sciences, v. 25, no. 1, p. 45–56, https://doi.org/10.1016/j.jseaes.2004.01.016.

Hirth, G., and Kohlstedt, D.L., 1996, Water in the oceanic upper mantle: Implications for rheology, melt extraction and the evolution of the lithosphere: Earth and Planetary Science Letters, v. 144, p. 93–108, https://doi.org/10.1016/0012-821X(96)00154-9.

Hu, J., Liu, L., Faccenda, M., Zhou, Q., Fischer, K.M., Marshak, S., and Lundstrom, C., 2018, Modification of the Western Gondwana craton by plume-lithosphere interaction: Nature Geoscience, v. 11, p. 203–210, https://doi.org/10.1038/s41561-018-0064-1.

Jia, C.Z., 1997, Tectonic Characteristics and Petroleum, Tarim Basin, China: Beijing, Petroleum Industry Press, 449 p.

Kincaid, C., Druken, K.A., Griffiths, R.W., and Stegman, D.R., 2013, Bifurcation of the Yellowstone plume driven by subduction-induced mantle flow: Nature Geoscience, v. 6, p. 395–399, https://doi.org/10.1038/ngeo1774.

Lee, C.T., Yin, Q., Rudnick, R.L., and Jacobsen, S.B., 2001, Preservation of ancient and fertile lithospheric mantle beneath the southwestern United States: Nature, v. 411, p. 69–73, https://doi.org/10.1038/35075048.

Lee, C.T.A., Luffi, P., and Chin, E.J., 2011, Building and destroying continental mantle: Annual Review of Earth and Planetary Sciences, v. 39, p. 59–90, https://doi.org/10.1146/annurev-earth-040610-133505.

Li, D.X., Yang, S.F., Chen, H.L., Cheng, X.L., Li, K., Jin, X.L., Li, Z.L., and Zou, S.Y., 2014, Late Carboniferous crustal uplift of the Tarim plate and its constraints on the evolution of the Early Permian Tarim large igneous province: Lithos, v. 204, p. 36–46, https://doi.org/10.1016/j.lithos.2014.05.023.

Liu, J., Xia, Q.K., Kuritani, T., Hanski, E., and Yu, H.R., 2017, Mantle hydration and the role of water in the generation of large igneous provinces: Nature Communications, v. 8, p. 1–8, https://doi.org/10.1038/s41467-017-01940-3.

Liu, M., and Furlong, K.P., 1994, Intrusion and underplating of mafic magmas: Thermal-rheological effects and implications for Tertiary tectonomagmatism in the North American Cordillera: Tectonophysics, v. 237, p. 175–187, https://doi.org/10.1016/0040-1951(94)90253-4.

Liu, Y.G., Lü, X.B., Wu, C.M., et al., 2016, The migration of Tarim plume magma toward the northeast in Early Permian and its significance for the exploration of PGE-Cu-Ni magmatic sulfide deposits in Xinjiang, NW China: As suggested by Sr-Nd-Hf isotopes, sedimentology and geophysical data: Ore Geology Reviews, v. 72, p. 538–545, https://doi.org/10.1016/j.oregeorev.2015.07.020.

Maus, S., Barckhausen, U., Berkenbosch, H., Bournas, N., et al., 2009, EMAG2: A 2-arc min resolution Earth Magnetic Anomaly Grid compiled from satellite, airborne, and marine magnetic measurements: Geochemistry Geophysics Geosystems, v. 10, Q08005, https://doi.org/10.1029/2009GC002471.

Neil, E.A., and Houseman, G.A., 1997, Geodynamics of the Tarim Basin and the Tian Shan in central Asia: Tectonics, v. 16, p. 571–584, https://doi.org/10.1029/97TC01413.

Roest, W.R., Verhoef, J., and Pilkington, M., 1992, Magnetic interpretation using the 3-D analytic signal: Geophysics, v. 57, p. 116–125, https://doi.org/10.1190/1.1443174.

Selway, K., Yi, J., and Karato, S.I., 2014, Water content of the Tanzanian lithosphere from magnetotelluric data: Implications for cratonic growth and stability: Earth and Planetary Science Letters, v. 388, p. 175–186, https://doi.org/10.1016/j.epsl.2013.11.024.

Wu, C., Yin, A., Zuza, A.V., Zhang, J., Liu, W., and Ding, L., 2016, Pre-Cenozoic geologic history of the central and northern Tibetan Plateau and the role of Wilson cycles in constructing the Tethyan orogenic system: Lithosphere, v. 8, p. 254–292, https://doi.org/10.1130/L494.1.

Xiao, W., Windley, B.F., Hao, J., and Zhai, M., 2003, Accretion leading to collision and the Permian Solonker suture, Inner Mongolia, China: Termination of the Central Asian orogenic belt: Tectonics, v. 22, 1069, https://doi.org/10.1029/2002TC001484.

Xiao, W.J., Windley, B.F., Liu, D.Y., Jian, P., Liu, C.Z., Yuan, C., and Sun, M., 2005, Accretionary tectonics of the Western Kunlun orogen, China: A Paleozoic–early Mesozoic, long-lived active continental margin with implications for the growth of southern Eurasia: The Journal of Geology, v. 113, p. 687–705, https://doi.org/10.1086/449326.

Xiong, S.Q., Tong, J., Ding, Y.Y., and Li, Z.K., 2016, Aeromagnetic data and geological structure of continental China: A review: Applied Geophysics, v. 13, p. 227–237, https://doi.org/10.1007/s11770-016-0552-2.

Xu, Y.G., Wei, X., Luo, Z.Y., Liu, H.Q., and Cao, J., 2014, The Early Permian Tarim large igneous province: Main characteristics and a plume incubation model: Lithos, v. 204, p. 20–35, https://doi.org/10.1016/j.lithos.2014.02.015.

Yang, H., Wu, G., Kusky, T.M., Chen, Y., and Xiao, Y., 2018, Paleoproterozoic assembly of the North and South Tarim terranes: New insights from deep seismic profiles and Precambrian granite cores: Precambrian Research, v. 305, p. 151–165, https://doi.org/10.1016/j.precamres.2017.11.015.

Yang, S.F., Chen, H.L., Dong, C.W., Jia, C.Z., and Wang, Z.G., 1996, The discovery of Permian syenite inside Tarim Basin and its geodynamic significance: Geochimica, v. 25, p. 121–128 [in Chinese].

Yin, A., and Harrison, T.M., 2000, Geologic evolution of the Himalayan-Tibetan orogen: Annual Review of Earth and Planetary Sciences, v. 28, p. 211–280, https://doi.org/10.1146/annurev.earth.28.1.211.

Yin, A., and Nie, S., 1996, A Phanerozoic palinspastic reconstruction of China and its neighboring regions, *in* Yin, A., and Harrison, T.M., eds., The Tectonics of Asia: New York, Cambridge University Press, p. 442–485.

Yin, A., Nie, S., Craig, P., Harrison, T.M., Ryerson, F.J., Xianglin, Q., and Geng, Y., 1998, Late Cenozoic tectonic evolution of the southern Chinese Tian Shan: Tectonics, v. 17, p. 1–27, https://doi.org/10.1029/97TC03140.

Zhang, D.Y., Zhang, Z.C., Santosh, M., Cheng, Z.G., Huang, H., and Kang, J.L., 2013, Perovskite and baddeleyite from kimberlitic intrusions in the Tarim large igneous province signal the onset of an end-Carboniferous mantle plume: Earth and Planetary Science Letters, v. 361, p. 238–248, https://doi.org/10.1016/j.epsl.2012.10.034.

Printed in USA